Circulation Journal
Official Journal of the Japanese Circulation Society
http://www.j-circ.or.jp

ORIGINAL ARTICLE
Arrhythmia/Electrophysiology

Molecular and Functional Changes in Voltage-Gated Na^+ Channels in Cardiomyocytes During Mouse Embryogenesis

Liangzhu Yu, MD; Shijun Gao, MD; Li Nie, MD; Ming Tang, MD; Weifeng Huang; Hongyan Luo; Xinwu Hu; Jiaoya Xi, MD; Minjie Zhu, MD; Yunjie Zheng, MD; Linlin Gao, MD; Lanqiu Zhang, MD; Yuanlong Song, MD; Jürgen Hescheler, MD; Huamin Liang, MD

Background: Embryonic cardiomyocytes undergo profound changes in their electrophysiological properties during development. However, the molecular and functional changes in Na^+ channel during cardiogenesis are not yet fully explained.

Methods and Results: To study the functional changes in the Na^+ channel during cardiogenesis, Na^+ currents were recorded in the early (EDS) and late (LDS) developmental stages of cardiomyocytes in embryonic mice. Compared with EDS myocytes, LDS myocytes exhibited a larger peak current density, a more negative shift in the voltage of half inactivation, a larger fast inactivation component and a smaller slow inactivation component, and smaller time constants for recovery from inactivation. Additionally, multiple Na^+ channel α-subunits (Nav 1.1–1.6) and β-subunits (Nav β1–β3) of mouse embryos were investigated. Transcripts of Nav 1.1–1.3 were absent or present at very low levels in embryonic hearts. Transcripts encoding Nav 1.4–1.6 and Nav β1–β3 increased during embryogenesis. Data on the sensitivity of total Na^+ currents to tetrodotoxin (TTX) showed that TTX-resistant Nav 1.5 is the predominant isoform expressed in the heart of the mouse embryo.

Conclusions: The results indicate that significant changes in the functional properties of Na^+ channels develop in the cardiomyocytes of the mouse embryo, and that different Na^+ channel subunit genes are strongly regulated during embryogenesis, which further support a physiological role for voltage-gated Na^+ channels during heart development. (*Circ J* 2011; **75:** 2071–2079)

Key Words: Cardiomyocytes; Electrophysiology; Embryogenesis; Na^+ channel

Voltage-gated sodium (Na^+) channels are composed of a pore-forming α-subunit and auxiliary β-subunits.[1] At least 6 α-subunits (Nav 1.1–1.6) and 4 β-subunits (Nav β1–β4) have been detected in the mammalian heart.[2,3] The different α-subunit isoforms have distinct electrophysiological and pharmacological properties.[1] Based on their sensitivity to tetrodotoxin (TTX), voltage-gated Na^+ channels are divided into TTX-sensitive and TTX-resistant channels. TTX-sensitive Na^+ channels are sensitive to nanomolar concentrations of TTX (IC_{50}, 1–25 nmol/L), including neuronal Nav 1.1, Nav 1.2, Nav 1.3, Nav 1.6 and skeletal muscle Nav 1.4.[1] In contrast, the predominant cardiac isoform (Nav 1.5) is inhibited by micromolar concentrations of TTX (IC_{50}, 2–6 μmol/L) and defined as a TTX-resistant channel.[1] Because of their distinct expression patterns and subcellular localizations, these isoforms have different functions.[4,5] The principal cardiac isoform, Nav 1.5, localized in the intercalated disks, is responsible for action potential conduction between cells, whereas neuronal Nav 1.1, Nav 1.3 and Nav 1.6 have been found in the transverse tubules, contributing to excitation–contraction coupling.[5] Although Na^+ channel α-subunits are sufficient to form functional channels when expressed alone, their kinetics and channel localization are tightly regulated by the β-subunits.[6–10]

Na^+ channels play an important role in the upstroke and conduction of the action potential in the heart. The orchestrated activation and inactivation of Na^+ channels is vital to normal myocardium function, and in maintaining normal heart

Received December 5, 2010; revised manuscript received March 18, 2011; accepted April 8, 2011; released online June 28, 2011
Time for primary review: 12 days

Chinese-German Stem Cell Center, Department of Physiology, Tongji Medical College, Huazhong University of Science and Technology, Wuhan (L.Y., S.G., L.N., M.T., W.H., H. Luo, X.H., J.X., M.Z., Y.Z., L.G., L.Z., Y.S., H. Liang), China; Institute of Neurophysiology, University of Cologne, Cologne (J.H.), Germany

The first two authors contributed equally to this work (L.Y., S.G.).

Mailing address: Huamin Liang, MD, Chinese-German Stem Cell Center, Department of Physiology, Tongji Medical College, Huazhong University of Science and Technology, Wuhan, 430030, China. E-mail: lianghuamin@hotmail.com

ISSN-1346-9843 doi:10.1253/circj.CJ-10-1212

Table. Primer Pairs Used for Reverse Transcription-Polymerase Chain Reaction

Gene	Primer sequence	Accession No.	Product size (bp)
Nav 1.1	F: 5'-tcatctcgctccgccattat-3'	NM018733.2	394
	R: 5'-gaggtggtgatttggaacagg-3'		
Nav 1.2	F: 5'-cttgcagtggcccccagaca-3'	NM001099298.2	363
	R: 5'-tcccagcagcacgcaaggtc-3'		
Nav 1.3	F: 5'-cggaaccaccagtggcgtgg-3'	NM018732.3	251
	R: 5'-cttctcggggcggagcaacg-3'		
Nav 1.4	F: 5'-gagggcttaccgccgccatc-3'	NM133199.2	381
	R: 5'-gccccgttccccaactctgc-3'		
Nav 1.5	F: 5'-tcacacactggggcgggaca-3'	NM021544.3	423
	R: 5'-accgctccctttgctgccac-3'		
Nav 1.6	F: 5'-agctggccgactttgccgac-3'	NM011323.2	211
	R: 5'-ttggacgccacgaaccgctc-3'		
Nav β1	F: 5'-cgctatgagaatgaggtgctg-3'	NM011322.2	145
	R: 5'-cgtagtcgccagagtggttg-3'		
Nav β2	F: 5'-ctaaggcttggtctggtggc-3'	NM001014761.2	124
	R: 5'-gctgatggctgttccctagc-3'		
Nav β3	F: 5'-aacttggttactcggttggg-3'	NM153522.2	129
	R: 5'-ttgaaaggaaagcctgagatag-3'		
GAPDH	F: 5'-aagcccatcaccatcttccaggag-3'	NM008084.2	308
	R: 5'-agcccttccacaatgccaaag-3'		

F, forward; R, reverse.

rhythm. Altered Na^+ channel properties may have important consequences for cardiac excitability and underlie multiple cardiac diseases, such as long QT syndrome,[11,12] Brugada syndrome,[13] idiopathic ventricular fibrillation,[14] and other cardiac conduction disorders.[15] The gain-of-function mutation in the gene encoding Nav 1.5 (SCN5A) is linked to long-QT syndrome,[13] whereas loss-of-function mutation in SCN5A is a cause of Brugada syndrome.[16] These considerations prompted a series of investigations aimed at determining molecular and functional changes in Na^+ channels in experimental and human models of cardiac diseases.

Fetal cardiomyocytes experience profound changes in their electrophysiological properties during development,[17–19] and sodium channels might be involved.[17] The purpose of this study was to use the patch-clamp technique to investigate the developmental changes in the functional properties of Na^+ channels in the cardiomyocytes of mouse embryos, and to use reverse transcription polymerase chain reaction (RT-PCR) determine changes in Na^+ channel subunits expression that might be associated with the functional changes.

Methods

Cell Isolation and Culture

Precisely staged pregnant Kunming mice (4–6 weeks old) were supplied by the Medical Experimental Animal Center, Tongji Medical College of Huazhong University of Science and Technology. For isolation of the different developmental stages of the cardiomyocytes, embryos aged 10.5–12.5 days post coitum and 16.5–18.5 days post coitum were respectively considered as the early developmental stage (EDS) and late developmental stage (LDS). Briefly, after the embryos were harvested, hearts were dissected and ventricles separated from atria, single cardiomyocytes were isolated from the ventricles using enzymatic dissociation procedures as described previously.[18,19] The isolated cells were plated onto sterile, gelatin-coated glass coverslips and kept in the incubator for 24–48 h. All procedures were performed in accordance with the Guidelines of the Hubei Council of Animal Care and approved by the Animal Use Subcommittee of Huazhong University of Science and Technology, China.

Patch-Clamp Recordings

The cells were placed in a temperature-controlled recording chamber that was mounted on the stage of an inverted microscope (Zeiss, Germany). Single, spontaneously beating ventricular cardiomyocytes were investigated with the whole-cell patch clamp technique in a conventional configuration at room temperature (22±2°C). For recordings, an Axopatch 200A patch-clamp amplifier (Molecular Devices, Sunnyvale, CA, USA) was used. Capacitance and series resistances were adjusted to obtain minimal contribution of the capacitive transients. Series resistance was compensated by 60–80% without ringing. Membrane currents were digitized at 10 kHz, filtered at 2 kHz, and stored on a hard drive for analysis. The patch pipettes had 1–2 MΩ tip resistance when filled with an intracellular pipette solution containing (in mmol/L): CsCl 120, $CaCl_2$ 1, $MgCl_2$ 5, Na_2ATP 5, tetraethylammonium 10, EGTA 11, HEPES 10 (pH 7.3 with CsOH). The bath solution contained (in mmol/L): NaCl 65, CsCl 70, $CaCl_2$ 1, $MgCl_2$ 1, $CdCl_2$ 0.05, glucose 10, HEPES 10 (pH 7.4 with CsOH).In all experiments, recording began approximately 20 min after establishment of the whole-cell mode to minimize the contribution of time-dependent shifts of steady-state gating parameter measurements.

Voltage Protocols

For the steady-state activation protocol, Na^+ currents were elicited by a series of 50-ms depolarizing pulses applied from a holding potential (HP) of –120 mV, in 10 mV increments between –90 and +60 mV. For steady-state activation curves, the Boltzmann equation was fitted to these data:

$$G/G_{max}=1/\{1+\exp[(V-V_{1/2})/k]\} \quad (1)$$

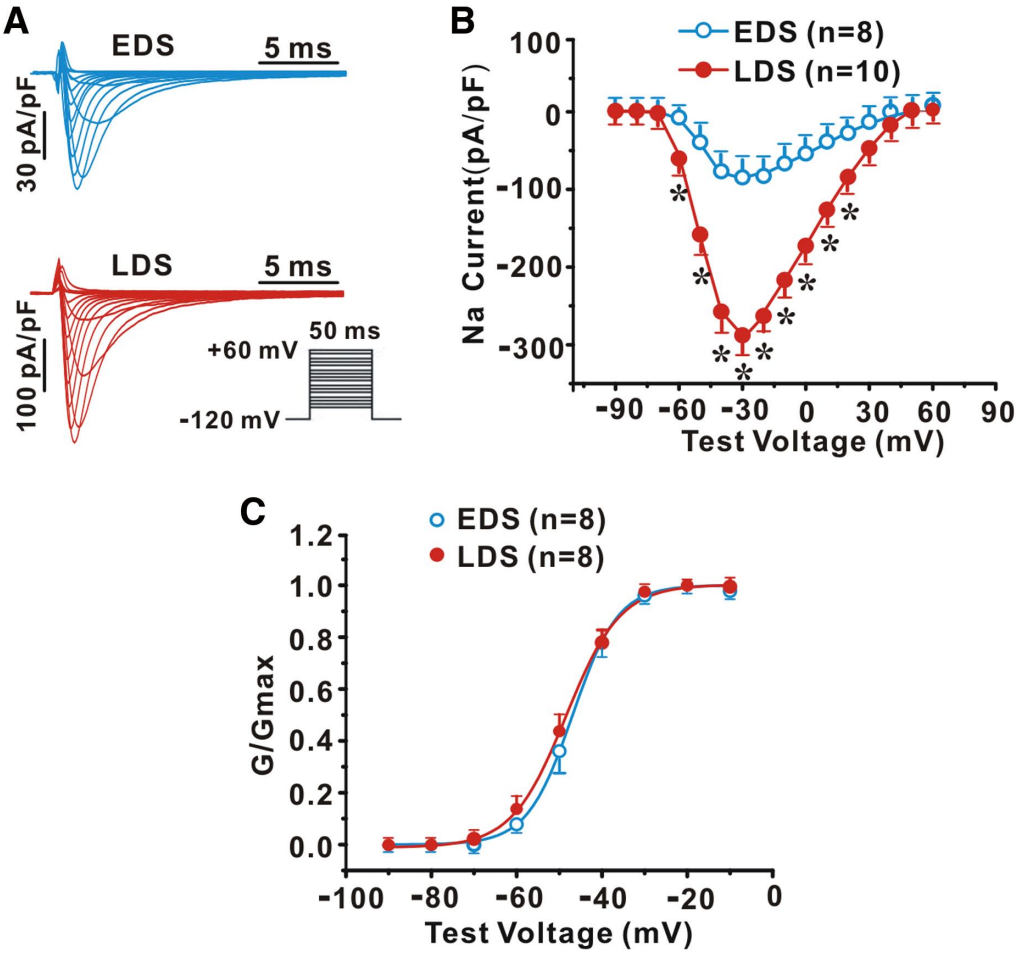

Figure 1. Current density and activation properties of Na^+ current in early (EDS) and late (LDS) development stage myocytes. (**A**) Representative Na^+ current traces for the peak current density–voltage (I–V) and activation curves. The voltage protocol is shown in the inset. Note the difference in the current amplitude scale between EDS and LDS myocytes. (**B**) Peak I–V curve. (**C**) Steady-state activation curve. *P<0.01 LDS vs. EDS cells. The number of cells is shown next to the symbols.

where G_{max} is the maximal peak Na^+ conductance, and $V_{1/2}$ and k are the voltage of half activation and slope factor, respectively.

The steady-state inactivation protocol was from a HP of –120 mV, a 500 ms conditioning prepulse applied in 5-mV increments between –130 and –30 mV, followed by a 20-ms test pulse to –20 mV. For steady-state inactivation curves, the following equation was fitted to these data to produce the least-squares fit curves:

$$I/I_{max} = 1/\{1+\exp[(V-V_{1/2})/k]\} \quad (2)$$

where $V_{1/2}$ is the voltage of half inactivation, and k is the slope factor.

The recovery from inactivation protocol was from a HP of –120 mV followed by a pulse to –20 mV (P1) for 500 ms, and then stepped to the recovery potential for 1–1,024 ms. After the recovery pulse, the potential was again stepped to –20 mV (P2) for 20 ms. The peak currents measured during the 2 –20 mV depolarizations were compared to produce the recovery fractional current (P2/P1). The fractional current was plotted as a function of the recovery time (in ms) between the 2 test pulses to –20 mV. The time course of recovery from inactivation was analyzed by a bi-exponential fitting using the equation:

$$P2/P1 = A_f\exp(-t/\tau_f) + A_s\exp(-t/\tau_s) + A_o \quad (3)$$

where A_f and A_s represent the relative fractions of the fast and slow recovery components, and τ_f and τ_s are the fast and slow recovery time constants, respectively.

To determine the inactivation time constants, the decay phase of the current during a voltage step was fitted with a bi-exponential function of the form:

$$I_{Na}/I_{Na,max} = A_f\exp(-t/\tau_f) + A_s\exp(-t/\tau_s) \quad (4)$$

where A_f and A_s are the relative amplitudes of the fast and slow inactivation components, and τ_f and τ_s are the fast and slow inactivation time constants, respectively.

RT-PCR

The mRNA expression of the Na^+ channel subunits was analyzed by RT-PCR. Total RNA was extracted from embryonic ventricular tissue using the RNeasy Mini-Kit (Qiagen GmbH, Germany) according to the manufacturer's protocol. RNA concentration was calculated by measuring absorbance at

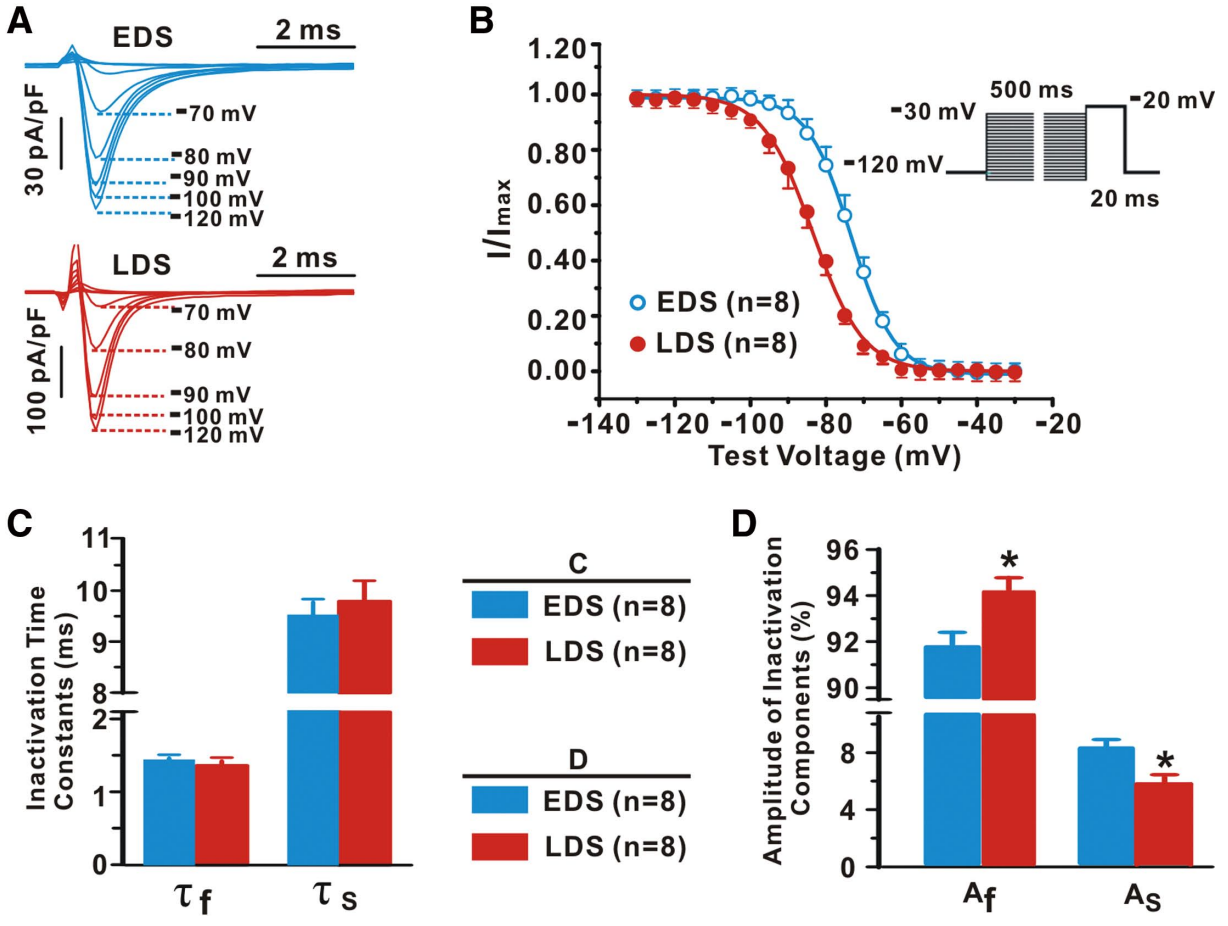

Figure 2. Inactivation properties of Na^+ current in early (EDS) and late (LDS) development stage myocytes. (**A**) Illustrative Na^+ current traces for the inactivation curve. (**B**) Steady-state inactivation curve of the Na^+ current. The voltage protocol is shown in the inset. (**C**) Mean values for the time constants of the fast (τ_f) and slow (τ_s) inactivation components at a test potential of –30 mV. (**D**) Mean values for the relative amplitudes (%) of the fast (A_f) and slow (A_s) inactivation components of the Na^+ current. *P<0.01 LDS vs. EDS cells. The number of cells is shown next to the symbols.

260 nm. cDNA was generated from 2 μg of total RNA using reverse transcriptase (Boehringer-Mannheim, Germany) and oligo (dT) primers (Boehringer-Mannheim, Germany). The RT reaction was carried out at 42°C for 1 h and at 95°C for 5 min. Products of the RT reaction were subjected to PCR amplifications using specific primers as listed in the **Table**. Single cells were picked up with a glass pipette and stored together with RNase inhibitor (Invitrogen GmbH, Germany) in PCR tubes and kept at –80°C, followed by standard protocols for further processing.

The amplification conditions included a denaturation of 3 min at 94°C, followed by 30 cycles of amplification (30 s at 94°C for denaturation, 30 s for annealing at 54°C for Nav 1.1 and Nav β1, 58°C for Nav β2 and Nav β3, 60°C for Nav 1.2, Nav 1.5 and Nav 1.6, 62°C for Nav 1.3 and Nav 1.4, and 30 s at 72°C for extension), and a final incubation of 10 min at 72°C. Forty cycles of amplification was performed for singe-cell RT-PCR.

The PCR products were stained with ethidium bromide, separated by 2% agarose gel electrophoresis, and examined by a bioimaging analyzer (BioRad, Richmond, CA, USA). The intensity values were normalized for GAPDH reference genes.

Single-Cell Real-Time PCR

Real-time PCR was performed on MxPRO3000 equipment (Stratagene Technology, USA) in a total reaction volume of 20 μl containing 10 μl SYBR Green Real-time PCR Master Mix (Toyobo, Japan), 0.4 μmol/L of each forward and reverse primer and 2 μl cDNA templates. The PCR processing consisted of 40 cycles of 10-s denaturation at 95°C, 20-s annealing at 60°C, and 15-s extension at 72°C. The primers were as follows: Nav 1.4: forward 5'-gagctgaaagacaatca-3', reverse 5'-ctgctgagcaagatcatgaa-3'; Nav 1.5: forward 5'- atggtcattg-gcaaccttgtggt-3', reverse 5'- ctgttctcttcatcctcttc-3'; Nav 1.6: forward 5'-agaagaagtactacaacgcc-3', reverse 5'-agtagtgtctcaa-ggcaaac-3'; GAPDH: forward 5'- catagacaagatggtgaatcgg-3', reverse 5'-gtccactttgtcacaagagaaggc-3'. The transcript expression levels were quantified by using the threshold cycle (Ct) value method, where values were normalized to GAPDH as an internal control in the same sample. The specificity of the PCR product amplification was confirmed by the melting curves.

Statistical Analysis

Data analysis was performed with Origin 7.5 software

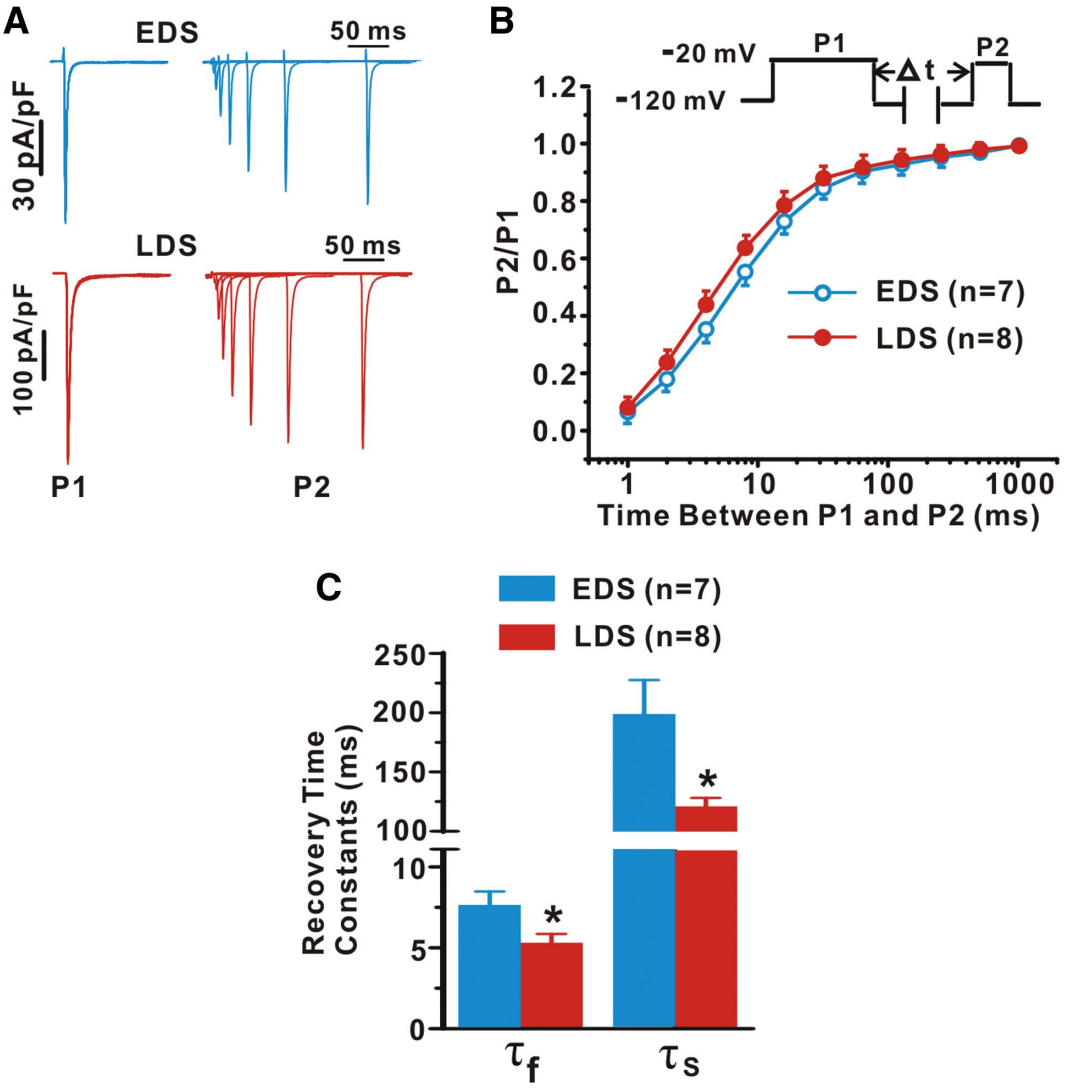

Figure 3. Recovery from inactivation in early (EDS) and late (LDS) development stage myocytes. (**A**) Representative Na^+ current traces for the recovery curve. The currents were elicited by 500 ms pulses to –20 mV (P1) with varying inter-pulse durations at a recovery potential of –120 mV and subsequent –20 mV test pulses (P2). (**B**) Recovery curve from inactivation of the Na^+ current. (**C**) Smaller time constants of the fast (τ_f) and slow (τ_s) recovery components were found in LDS than in EDS myocytes. *P<0.01 LDS vs. EDS cells. The number of cells is shown next to the symbols.

(Microcal Software, USA) and Clampfit 9.0 software (Axon Instruments, USA). All data are expressed as mean±SEM. Unpaired t-tests and 1-way ANOVA were performed where appropriate. A statistically significant difference was defined as P<0.05.

Results

Developmental Changes in Peak Current Density and Gating Properties of Na^+ Channels During Mouse Embryogenesis

Activation As illustrated in Figures 1A,B, the peak Na^+ current density was significantly larger in the LDS cells (n=10; –60 to +20 mV) than in the EDS cells (n=8) (P<0.01), indicating that the Na^+ current density increased significantly during development. However, the voltage dependence of activation in both cell types was similar (Figure 1C). There was no significant difference in the voltage of half activation ($V_{1/2}$) or slope factor (k) between EDS and LDS myocytes ($V_{1/2}$: –46.1±3.4 mV EDS vs. –47.0±3.4 mV LDS, P>0.05; k: 5.5±0.4 mV EDS vs. 5.8±0.7 mV LDS, P>0.05).

Inactivation Figures 2A,B shows the representative Na^+ currents and steady-state inactivation curves. We found that the voltage of half inactivation ($V_{1/2}$) shifted to a more negative potential in the LDS (n=8) compared with the EDS (n=8) cells ($V_{1/2}$: –82.7±4.4 mV LDS vs. –71.6±2.4 mV EDS, P<0.01). The k values for the EDS and LDS cells were not significantly different (7.2±0.7 mV EDS vs. 6.5±0.9 mV LDS, P>0.05). To compare the time-dependence of Na^+ channel inactivation in EDS and LDS cardiomyocytes, the time constants and relative amplitudes of fast (τ_f, A_f) and slow (τ_s, A_s) inactivation components at a test potential of –30 mV were shown in Figures 2C,D. The time constants of Na^+ channel

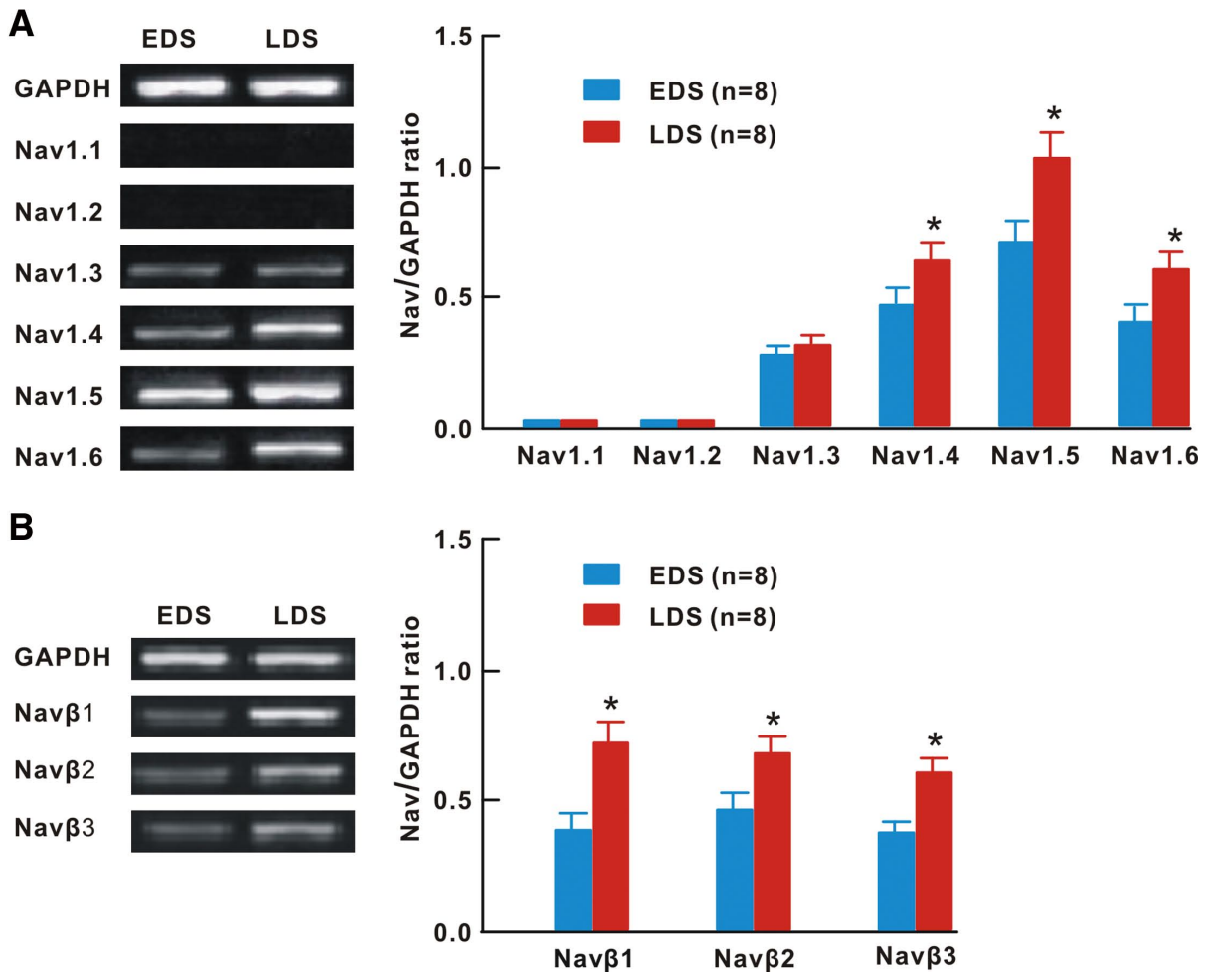

Figure 4. Expression of different Na^+ channel subunits in early (EDS) and late (LDS) development stage ventricles. (**A**) Expression of 6 Na^+ channel α-subunits at the mRNA level in EDS and LDS ventricles. (**B**) Expression of 3 Na^+ channel β-subunits at the mRNA level in EDS and LDS ventricles. Relative expression levels of the mRNA of different Na^+ channel subunits quantified as described in the Methods. *P<0.01 LDS vs. EDS cells. The number of cells is shown next to the symbols.

inactivation in both cell types were similar (P>0.05). But LDS myocytes had significantly larger amplitude of fast (A_f) inactivation components than in EDS myocytes (A_f: 94.1±0.1% LDS vs. 91.7±0.1% EDS, P<0.01; A_s: 5.9±0.1% LDS vs. 8.2±0.1% EDS, P<0.01).

Recovery From Inactivation Figures 3A,B shows illustrative currents and the recovery curves from inactivation. We found that both the fast (τ_f) and the slow (τ_s) time constants for Na^+ channel recovery were significantly smaller in LDS (n=8) (τ_f: 5.5±0.4 ms LDS vs. 7.5±0.5 ms EDS, P<0.01; τ_s: 122.5±4.5 ms LDS vs. 198.6±12.3 ms EDS, P<0.01) than in EDS (n=7) cells (Figure 3C).

Expression of Na^+ Channel α- and β-Subunits in Embryonic Cardiomyocytes

Expressions of the Nav 1.1–1.6 subunits at different stages of development were investigated. The amount of Nav 1.4, Nav 1.5 and Nav 1.6 in whole ventricle tissue increased with age during ontogeny. Transcripts of Nav 1.1, Nav 1.2 and Nav 1.3 were absent or present at very low levels in embryonic ventricles (Figure 4A). The expression pattern of the various Na^+ channel α-subunits in the present study is similar to that in the postnatal mouse heart.[2] The expressions of 3 Na^+ channel β-subunits (Nav β1–β3) were upregulated in whole ventricles during embryogenesis (Figure 4B). Because of the lack of evidence for its regulation of Na^+ channels, Nav β4 was not investigated in the present study.

To exclude contamination by other cell types, single cell RT-PCR was performed to demonstrate the expression pattern of different Na^+ channel subunits in ventricular cardiomyocytes. Similar developmental changes as revealed in the whole ventricles were found in each subunit. At the EDS, only Nav 1.5 and Nav β1 were detectable whereas at the LDS low expressions of Nav 1.4, Nav 1.6, Nav β2 and Nav β3 were observed (Figure 5A). The single-cell real-time PCR experiments demonstrated that Nav 1.5 was the most abundant subunit in both EDS and LDS myocytes (Figure 5B). The expressions of Nav 1.4, Nav 1.5 and Nav 1.6 mRNA significantly increased during embryogenesis according to the following: Nav 1.5>>Nav 1.4>Nav 1.6.

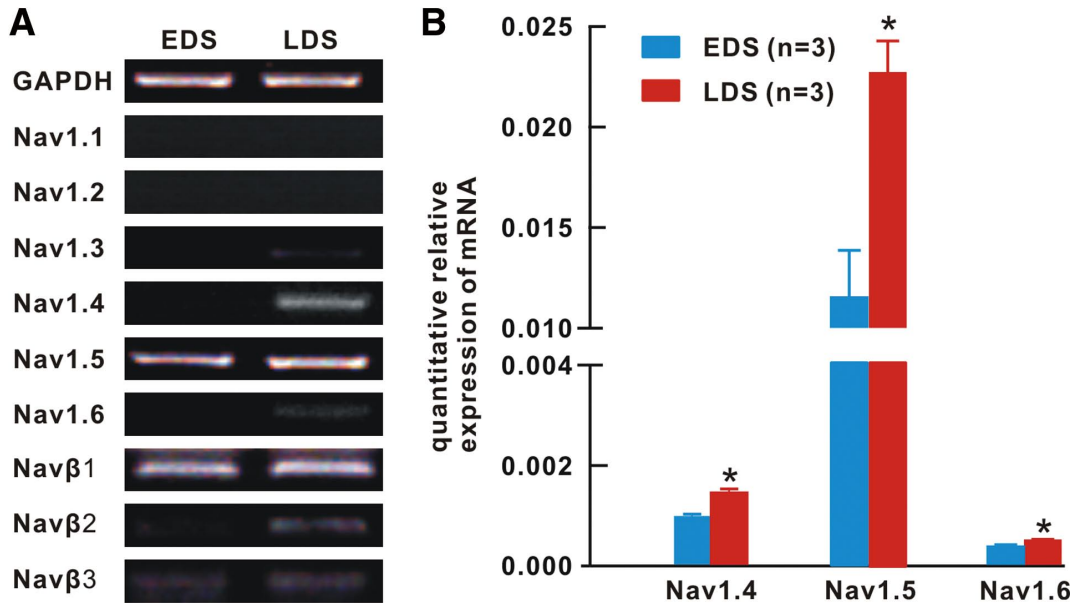

Figure 5. Expression of different Na^+ channel subunits in single beating early (EDS) and late (LDS) development stage myocytes. (**A**) Expression of different Na^+ channel subunits measured by single-cell reverse transcription-polymerase chain reaction. (**B**) Relative expression levels of Nav 1.4, Nav 1.5 and Nav 1.6 measured by single-cell real-time polymerase chain reaction. *P<0.01 LDS vs. EDS cells. The number of cells is shown next to the symbols.

Sensitivity of Total Na^+ Currents to TTX

Finally, to determine the sensitivity of the total Na^+ current in both embryonic cardiomyocyte types, we performed whole-cell voltage clamp experiments in the presence of TTX at concentrations from 0.1 to 50 μmol/L. Currents during 50-ms depolarizations to –30 mV from a holding potential of –100 mV were decreased by TTX in a dose-dependent manner in both myocyte types. Fitting the dose–response relationship with a Hill curve (Hill coefficient of 1) yielded an IC_{50} of 5.2 μmol/L (EDS, n=6) and 6.6 μmol/L (LDS, n=5–8) (**Figure 6**), which were within or very close to the micromolar range (2–6 μmol/L) reported previously.[1] Thus, the total Na^+ currents in both EDS and LDS myocytes primarily exhibited the TTX-resistant characteristic.

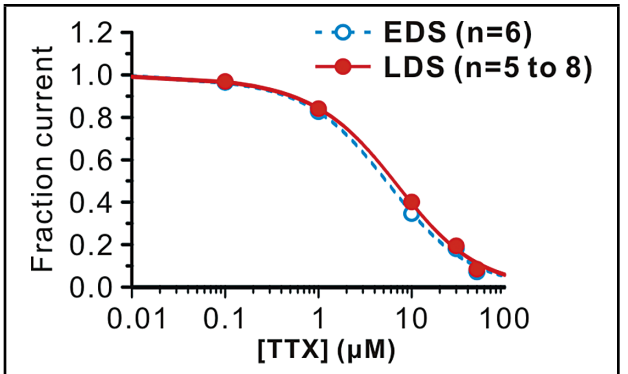

Figure 6. Dose–response curves of TTX blockage of total Na^+ currents in early (EDS) and late (LDS) development stage myocytes. Mean±SEM. The data are fitted with a Hill-type curve: fractional blockage = 1/(1+[TTX]/IC_{50}) with an IC_{50} of 5.2 μmol/L (EDS) and 6.6 μmol/L (LDS). TTX, tetrodotoxin. The number of cells is shown next to the symbols.

Discussion

There are 3 significant findings from the present study. (1) There are significant changes in the functional properties of Na^+ channels in cardiomyocytes during mouse embryogenesis. Cardiomyocytes at the LDS exhibits a negative shift in the voltage dependence of inactivation, a larger fast inactivation component and a smaller slow inactivation component, and an accelerated rate of recovery from inactivation. (2) There is marked upregulation of Na^+ channel subunits Nav 1.4, Nav 1.5, Nav 1.6, Nav β1, Nav β2, and Nav β3. (3) There is a similar sensitivity of the total Na^+ current to micromolar concentrations of TTX during cardiac development.

Functional Implications of Altered Na^+ Channel Properties

The developmental increase in peak I_{Na} density in the present study was in agreement with the fact that during the development of the murine heart, the maximum upstroke velocity (V_{max}) of the action potential increased.[20,21]

The hyperpolarizing shift in voltage-dependent inactivation combined with unaltered activation gave rise to a reduced overlap between the activation and inactivation curves, and hence a decrease in the persistent Na^+ current.[22,23] This persistent Na^+ current was believed to contribute to the action potential plateau and play an important role in the pathological changes in electrical excitability associated with many disease states, including cardiac arrhythmias, ischemic stroke, and epilepsy.[24] This is another explanation for the ongoing shortening of the action potential duration with maturation.[25] Although the time course of inactivation at both developmental stages had similar time constants, a larger fast inactiva-

tion component and a smaller slow inactivation component were found in cardiomyocytes at the LDS, which reflected a switch between different gating modes of the cardiac Na^+ channel.[26,27] Cardiomyocytes at the LDS also exhibited a more rapid time course of recovery from inactivation than those in the early stage. The faster recovery from inactivation combined with similar rate of fast inactivation may promote greater sodium conductance per unit time, and contribute to the increase in Na^+ current density.[28]

Expression Pattern of Na^+ Channel α-Subunits of Cardiomyocytes

In the present study, both the data from single cardiomyocytes and whole ventricles demonstrated developmental changes in the expression of different Na^+ channel α-subunits. Although the expressions of Nav 1.1, Nav 1.2 and Nav 1.3 mRNA were absent or present at very low levels, Nav 1.4, Nav 1.5 and Nav 1.6 were increased during cardiogenesis. Our results provided, to our knowledge, the first evidence of the expression of neuronal Na^+ channels (Nav 1.3, Nav 1.6) and the skeletal muscle Na^+ channel (Nav 1.4) in the embryonic mouse heart as early as 10.5 days post coitum.

Unlike the data from the whole ventricles, single-cell RT-PCR showed that EDS myocytes exclusively expressed Nav 1.5 and those in the LDS expressed mainly Nav 1.5 with minor expressions of Nav 1.4 and Nav 1.6. These findings strongly indicated that the data acquired from the whole ventricles had been contaminated by that for other cell types, such as fibroblasts and nerve cells. These cell types in cardiac tissues have been reported to express functional Na^+ channels.[29,30] Additionally, single-cell real-time PCR demonstrated upregulation of Nav 1.4, Nav 1.5 and Nav 1.6 during development.

Characterization of Total Na^+ Currents in Embryonic Ventricular Cardiomyocytes

Although our results showed the developmental expression of Nav 1.3, Nav 1.4 and Nav 1.6 in embryonic ventricular cardiomyocytes, the TTX-sensitive Na^+ current characteristic was not detected under our recording conditions. The total Na^+ currents in both EDS and LDS myocytes were sensitive to micromolar concentrations of TTX. Moreover, 0.1 μmol/L TTX reduced the total Na^+ current by 3.5±1.1% in EDS cells and 4.2±1.9% in LDS cells, which might represent an upper limit on the percentage of TTX-sensitive Na^+ currents, because this concentration of TTX was reported to specifically block the TTX-sensitive Na^+ channel without significantly affecting the TTX-resistant Nav 1.5 channel.[31] Real-time PCR in the present study also showed that Nav 1.5 was the most abundant subunit in both EDS and LDS myocytes, although at the LDS there were minor expressions of Nav 1.4 and Nav 1.6. Thus, our results showed that the TTX-resistant Nav 1.5 was the predominant isoform expressed in the heart of the mouse embryo.

In this study, the voltage-dependent activation in cardiomyocytes did not change significantly during embryogenesis, whereas the voltage-dependent inactivation shifted in the hyperpolarizing direction. The TTX-sensitive Na^+ current was reported to activate and inactivate at more positive potentials than the TTX-resistant Na^+ current,[5,31] so we assumed that the TTX-sensitive Na^+ current was a very small proportion of the total Na^+ currents and had little or no effect on the electrophysiological characteristics of total Na^+ current in the embryonic cardiomyocytes, which might explain the absence of a change in voltage-dependent activation during embryogenesis. Our findings were supported by previous studies showing that the fraction of the TTX-sensitive Na^+ current in most cardiac preparations was from 5% to 30%.[2,5,31,32] In addition, Bretteet al[4] also demonstrated a TTX-sensitive Na^+ current that accounted for 14±3% of the total Na^+ current and might not be required for normal excitation–contraction coupling in rat ventricular myocytes.

Functional Role of Na^+ Channel β-Subunits

One of the most prominent findings in the present study was the significant upregulation of accessory β-subunits during mouse embryogenesis. The upregulation of Nav β1 subunit mRNA was in line with the results of a previous study.[33] To date, we have been the first to reveal the expression of the Nav β2 and Nav β3 subunits in the embryonic heart.

Most studies found that coexpression of the Nav β1 subunit with the Nav 1.5 subunit increased the Na^+ current density, accelerated the rate of recovery from inactivation, and caused a negative or positive shift in steady-state inactivation with no effect on voltage-dependent activation, as well as hastening the rate of inactivation,[7,9,34,35] whereas coexpression of either the Nav β2 or Nav β3 with Nav 1.5 caused only changes in the kinetics of voltage-dependent activation and inactivation.[7–9] Thus, based on published studies of the effect of coexpression of accessory Nav β-subunits on the Na^+ current, we speculate that the increase in the 3 Nav β-subunits, together with upregulation of Nav 1.5, may contribute to the phenotypic changes in the electrophysiological characteristics of Na^+ currents during cardiac development.

Study Limitations

In this study, the technique to detect the expression of the Na^+ channel subunits was of paramount importance, because it was crucial for quantitative analysis of the functional channels. Although RT-PCR, used in this study, was valuable for predicting the expression pattern of different Na^+ channel subunits, it would be much better to perform Western blot analysis to examine the expression of these subunits at the protein level. In addition, we did not attempt to analyze the subcellular localization of these subunits by use of immunohistochemistry, which was another limitation of this study.

Taken together, our results illustrate significant functional and molecular changes in Na^+ channels during murine cardiogenesis. Cardiomyocytes derived from embryonic stem cells (ESCM) have potential both as an experimental model for investigating cardiac physiology and as a source for cardiac tissue repair.[36,37] The results obtained from the present study not only illustrate the characteristics of the Na^+ currents in mouse cardiomyocytes during normal embryonic development, but also provide a baseline against which research on ESCM may be compared. Moreover, these findings extend our understanding of the role performed by Na^+ channels during embryogenesis, indicating that there is considerable complexity and diversity of expression patterns, which may underlie functional significance.

Acknowledgments

This work was supported by a grant from the National Nature Science Foundation of China (NSFC grant no. 30700262) for Huamin Liang, another NSFC grant for Linlin Gao (no. 30670854), and a grant assisted by the Science Foundation of Huazhong University of Science and Technology (no. 2010MS052) for Huamin Liang.

References

1. Goldin AL. Resurgence of sodium channel research. *Annu Rev*

Physiol 2001; **63:** 871–894.
2. Haufe V, Camacho JA, Dumaine R, Gunther B, Bollensdorff C, von Banchet GS, et al. Expression pattern of neuronal and skeletal muscle voltage-gated Na^+ channels in the developing mouse heart. *J Physiol* 2005; **564:** 683–696.
3. Kaufmann SG, Westenbroek RE, Zechner C, Maass AH, Bischoff S, Muck J, et al. Functional protein expression of multiple sodium channel alpha- and beta-subunit isoforms in neonatal cardiomyocytes. *J Mol Cell Cardiol* 2009; **48:** 261–269.
4. Brette F, Orchard CH. No apparent requirement for neuronal sodium channels in excitation-contraction coupling in rat ventricular myocytes. *Circ Res* 2006; **98:** 667–674.
5. Maier SK, Westenbroek RE, Schenkman KA, Feigl EO, Scheuer T, Catterall WA. An unexpected role for brain-type sodium channels in coupling of cell surface depolarization to contraction in the heart. *Proc Natl Acad Sci USA* 2002; **99:** 4073–4078.
6. DharMalhotra J, Chen C, Rivolta I, Abriel H, Malhotra R, Mattei LN, et al. Characterization of sodium channel alpha- and beta-subunits in rat and mouse cardiac myocytes. *Circulation* 2001; **103:** 1303–1310.
7. Fahmi AI, Patel M, Stevens EB, Fowden AL, John JE 3rd, Lee K, et al. The sodium channel beta-subunit SCN3b modulates the kinetics of SCN5a and is expressed heterogeneously in sheep heart. *J Physiol* 2001; **537:** 693–700.
8. Johnson D, Bennett ES. Isoform-specific effects of the beta2 subunit on voltage-gated sodium channel gating. *J BiolChem* 2006; **281:** 25875–25881.
9. Ko SH, Lenkowski PW, Lee HC, Mounsey JP, Patel MK. Modulation of Na(v)1.5 by beta1- and beta3-subunit co-expression in mammalian cells. *Pflugers Arch* 2005; **449:** 403–412.
10. Zimmer T, Benndorf K. The intracellular domain of the beta 2 subunit modulates the gating of cardiac Nav 1.5 channels. *Biophys J* 2007; **92:** 3885–3892.
11. Viswanathan PC, Balser JR. Inherited sodium channelopathies: A continuum of channel dysfunction. *Trends Cardiovasc Med* 2004; **14:** 28–35.
12. Makita N. Phenotypic overlap of cardiac sodium channelopathies: Individual-specific or mutation-specific? *Circ J* 2009; **73:** 810–817.
13. Veldkamp MW, Viswanathan PC, Bezzina C, Baartscheer A, Wilde AA, Balser JR. Two distinct congenital arrhythmias evoked by a multidysfunctional Na(+) channel. *Circ Res* 2000; **86:** E91–E97.
14. Wan X, Chen S, Sadeghpour A, Wang Q, Kirsch GE. Accelerated inactivation in a mutant Na(+) channel associated with idiopathic ventricular fibrillation. *Am J Physiol Heart CircPhysiol* 2001; **280:** H354–H360.
15. Wang DW, Viswanathan PC, Balser JR, George AL Jr, Benson DW. Clinical, genetic, and biophysical characterization of SCN5A mutations associated with atrioventricular conduction block. *Circulation* 2002; **105:** 341–346.
16. Balser JR. Sodium "channelopathies" and sudden death: Must you be so sensitive? *Circ Res* 1999; **85:** 872–874.
17. Davies MP, An RH, Doevendans P, Kubalak S, Chien KR, Kass RS. Developmental changes in ionic channel activity in the embryonic murine heart. *Circ Res* 1996; **78:** 15–25.
18. Liang HM, Tang M, Liu CJ, Luo HY, Song YL, Hu XW, et al. Muscarinic cholinergic regulation of L-type calcium channel in heart of embryonic mice at different developmental stages. *ActaPharmacol Sin* 2004; **25:** 1450–1457.
19. Song GL, Tang M, Liu CJ, Luo HY, Liang HM, Hu XW, et al. Developmental changes in functional expression and beta-adrenergic regulation of I(f) in the heart of mouse embryo. *Cell Res* 2002; **12:** 385–394.
20. Liu W, Yasui K, Arai A, Kamiya K, Cheng J, Kodama I, et al. Beta-adrenergic modulation of L-type Ca^{2+}-channel currents in early-stage embryonic mouse heart. *Am J Physiol* 1999; **276:** H608–H613.
21. Yasui K, Liu W, Opthof T, Kada K, Lee JK, Kamiya K, et al. I(f) current and spontaneous activity in mouse embryonic ventricular myocytes. *Circ Res* 2001; **88:** 536–542.
22. Attwell D, Cohen I, Eisner D, Ohba M, Ojeda C. The steady state TTX-sensitive ("window") sodium current in cardiac Purkinje fibres. *Pflugers Arch* 1979; **379:** 137–142.
23. Baruscotti M, DiFrancesco D, Robinson RB. A TTX-sensitive inward sodium current contributes to spontaneous activity in newborn rabbit sino-atrial node cells. *J Physiol* 1996; **492:** 21–30.
24. Saint DA. The cardiac persistent sodium current: An appealing therapeutic target? *Br J Pharmacol* 2008; **153:** 1133–1142.
25. Yokoshiki H, Tohse N. Developmental changes of ion channels. *In*: Sperelakis N, Kurachi Y, Terzic A, Cohen MV, editors. Heart physiology and pathophysiology. 4th edn. New York: Academic Press, 2001: 719–735.
26. Bohle T, Benndorf K. Voltage-dependent properties of three different gating modes in single cardiac Na^+ channels. *Biophys J* 1995; **69:** 873–882.
27. Bohle T, Steinbis M, Biskup C, Koopmann R, Benndorf K. Inactivation of single cardiac Na^+ channels in three different gating modes. *Biophys J* 1998; **75:** 1740–1748.
28. Nguyen TP, Wang DW, Rhodes TH, George AL Jr. Divergent biophysical defects caused by mutant sodium channels in dilated cardiomyopathy with arrhythmia. *Circ Res* 2008; **102:** 364–371.
29. Li GR, Sun HY, Chen JB, Zhou Y, Tse HF, Lau CP. Characterization of multiple ion channels in cultured human cardiac fibroblasts. *PLoS One* 2009; **4:** e7307.
30. Tobin AE, Cruz-Bermudez ND, Marder E, Schulz DJ. Correlations in ion channel mRNA in rhythmically active neurons. *PLoS One* 2009; **4:** e6742.
31. Lei M, Jones SA, Liu J, Lancaster MK, Fung SS, Dobrzynski H, et al. Requirement of neuronal- and cardiac-type sodium channels for murine sinoatrial node pacemaking. *J Physiol* 2004; **559:** 835–848.
32. Haufe V, Cordeiro JM, Zimmer T, Wu YS, Schiccitano S, Benndorf K, et al. Contribution of neuronal sodium channels to the cardiac fast sodium current I_{Na} is greater in dog heart Purkinje fibers than in ventricles. *Cardiovasc Res* 2005; **65:** 117–127.
33. Dominguez JN, Nav arro F, Franco D, Thompson RP, Aranega AE. Temporal and spatial expression pattern of beta1 sodium channel subunit during heart development. *Cardiovasc Res* 2005; **65:** 842–850.
34. Baroudi G, Carbonneau E, Pouliot V, Chahine M. SCN5A mutation (T1620M) causing Brugada syndrome exhibits different phenotypes when expressed in *Xenopus* oocytes and mammalian cells. *FEBS Lett* 2000; **467:** 12–16.
35. Nuss HB, Chiamvimonvat N, Perez-Garcia MT, Tomaselli GF, Marban E. Functional association of the beta 1 subunit with human cardiac (hH1) and rat skeletal muscle (mu 1) sodium channel alpha subunits expressed in *Xenopus* oocytes. *J Gen Physiol* 1995; **106:** 1171–1191.
36. Tang XL, Rokosh DG, Guo Y, Bolli R. Cardiac progenitor cells and bone marrow-derived very small embryonic-like stem cells for cardiac repair after myocardial infarction. *Circ J* 2010; **74:** 390–404.
37. Mignone JL, Kreutziger KL, Paige SL, Murry CE. Cardiogenesis from human embryonic stem cells. *Circ J* 2010; **74:** 2517–2526.